

# **Cruise Report**

## **F.S. ALKOR Cruise No. 423**

**Dates of Cruise: 16. September to 18. September 2013**

**Projects:**  
**Student course in phys. oceanogr.**

Areas of Research: Physical oceanography

Port Call: no

Institute: Helmholtz Centre for Ocean Research Kiel GEOMAR

Chief Scientist: Dr. Johannes Karstensen

Number of Scientists: 12

Master: Norbert Hechler

# Chapter 1

## Scientific personal

Cruise code: AL 423

Cruise dates: 16.9. – 18.09.2013

Port call: Kiel – Kiel

Table 1.1: Scientific personal: GEOMAR: Helmholtz-Centre for Ocean Research Kiel, Kiel, Germany; CAU: Christian Albrechts Universität Kiel, Kiel, Germany

Name	Institute	Function
Johannes Karstensen	GEOMAR	Chief scientist
Christian Begler	GEOMAR	PO
Till Baumann	CAU	Master student
Eike Eduard Köhn	CAU	student
Thilo Klenz	CAU	student
Marcel Tesch	CAU	student
Hendrik Huster	CAU	student
Bodil Rühs	CAU	student
Sönke Hermann	CAU	student
Felix Grote	CAU	student
Maren E. Richter	CAU	student
Rene Schubert	CAU	student

Responsible for Report:

Johannes Karstensen

phone: ++49 (0)431 600-4156, fax: ++49 (0)431 600-4152

Helmholtz Centre for Ocean Research Kiel GEOMAR

Düsternbrooker Weg 20, 24105 Kiel, Germany

e-mail: jkarstensen@geomar.de

# Chapter 2

## Objective

The main purpose of the FS ALKOR cruise 423 was the training of students in observational methods for physical oceanographers. Undergraduate students in the Bachelor program "Physik des Erdsystems" are introduced into modern observational techniques in physical oceanography, including instrument calibration and interpretation of observations. The course (MNF-Pher-110b) is part of the "Messmethoden" lecture. The cruise provide to the students an opportunity to experience the work and life at sea and also to explore and investigate physical oceanography processes in the western Baltic Sea, the ocean at their backyard.

The scientific motivation of the cruise is to obtain a rather synoptic picture of the hydrography and water movement in the western Baltic. Hydrographic and current sections from the Fehmarn Belt (section C) and along the deepest topography from about 10°40 E to 14°21 E (section L) were done. Moreover, a long time mooring site that monitors the flow through the Fehmarn Belt is serviced.

# Chapter 3

## Cruise Narrative

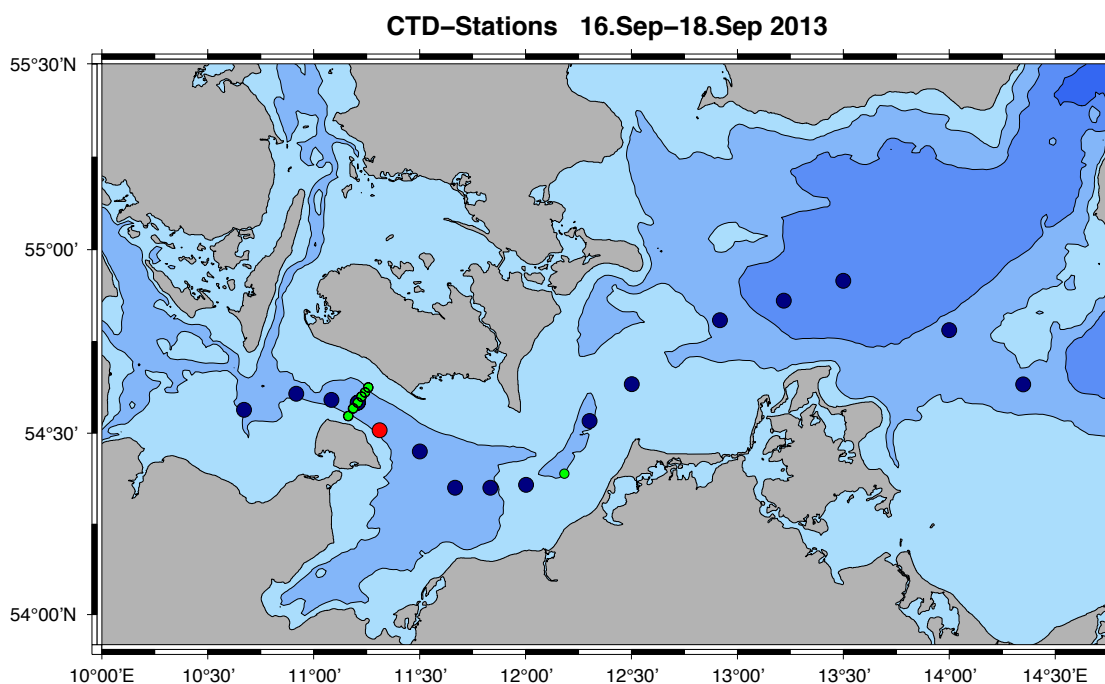


Figure 3.1: *FS ALKOR 423* cruise stations. Black (LG section)/ Green (FB section) and Red dot are the CTD stations, red dot is also location of the V431 mooring.

DAY 1 (Monday, 16.09.2013):

We left Kiel Westufer at 08:15 (all times in the cruise narrative are local time Kiel). The equipment (vmADCP 600kHz, Salinometer, PC etc.) was installed on Sunday morning (loaded on Saturday on the east shore pier). Shortly after leaving the port, the first officer, did a safety instruction and familiarization on board. A short introduction of the planned program for the following days was given. Ship ADCP (hull mounted 600kHz) and TSG were switched on. We headed for the first CTD test station, which was started at 10:45. The sensors showed expected values, only the bottle sampler did not work as expected - but this issue was quickly resolved.

Three more stations in the 'L' section were occupied, the last one in the Speergebiet, Marienleuchte, where the mooring is located. The mooring was released and the upper element appeared just a couple of minutes later at the surface. However, the recovery turned out to be difficult because of the wind making the manoeuvrability of the ship difficult. With the second attempt the upper floatation was saved aboard - while the anchor part connection detached. The rope broke off, very likely at the connection. It is not possible to recover the mooring frame and we have to ask for support from divers, e.g. RV DENEBO.

Next was an occupation of the C section (over the Fehmarn Belt) followed by a 7kn steaming along the same track for more precise ADCP measurements. After two other CTD profiles from the 'L' section we stopped the CTD work and steamed overnight to our easternmost position to start an occupation of the 'L' section from the east on Tuesday morning.

DAY 2 (Tuesday, 17.09.2013):

At 07:00 we started with the CTD work again by occupying station 21, the farthest east. The weather was surprisingly good (low wind, not much wave) compared to the forecast as well as to the reports we heard from Kiel. The whole day, until 21:00 we performed CTD stations along the L section. In parallel the students worked on the exercises and the salinometer was introduced to them and all did measurements. Unfortunately there were issues with the salinometer pump and we had to find a way in filling the cell with support from gravity. During the whole day the meteorological observations were done every 1 hour. During the night we found shelter in lee of the island of Fehmarn.

DAY 3 (Wednesday, 18.09.2013):

As the mooring could not be deployed because the bottom frame was still at the ground, we started at 08:00 with the re-occupation of the C section, crossing the Fehmarn Belt. This followed an ADCP occupation. At 10:00 we headed back to Kiel. At 14:42 we were moored at Kiel Westufer pier. All equipment stowed away during the passage was unloaded.

# Chapter 4

## Preliminary results

### 4.1 Hydrographic and currents along C and L section

#### Fehmarn Belt (C section)

The hydrology of Fehmarn Belt was measured twice during the cruise. Each time, six CTD profiles were taken between 54°32.8 N, 11°09.8E and 54°37.5N, 11°15.5E.

The temperature distribution (Figure 2) within the upper 19m of the Fehmarnbelt is nearly homogeneously 15-16°C. In 20m depth the water cools down with a very weak gradient to 14°C. Caused by cold bottom water at 11°C, the temperature gradient below 23m depth is stronger. Two days later the water is already cooled down. The temperature of the surface water is only 15°C in average and the maximum can be found in 13 to 14m depths with a temperature of 16°C. With increasing water depth, the temperature decreases constantly with weak gradients until it reaches 11°C at the bottom. The temperature of the bottom water did not change. The salinity distribution shows differences between north and south. In the north are weaker gradients at smaller depths and the surfaces value (12 psu) is less than the surfaces value of the south (14 psu). The first gradient is at 12m depth in the north and at 15m in the south. Here the salinity changes from 14 to 16 psu. The second and stronger gradient can be found in 16m where the salinity changes to 20 psu. So in general the salinity increases with depths and gets its maximum (24 psu) at the bottom. This salinity maximum can be identified as a salty North Sea water inflow.

The salinity distribution changed a lot compared to the situation two days ago. Caused by strong southwest winds the water mixes so there are not many differences between north and south anymore. Now there is a homogeneous surface layer (12) up to 14m depth. From 14 to 17m depths the salinity increases rapidly until it reaches 21 at 18m depth. Within the last 8m down to the bottom the salinity increases more slowly again and reaches 24 at the bottom in 26m depth. This is the same bottom salinity like two days before. The density distribution is very similar to the salinity distribution and has the same gradients and it also increases with depths. It changes from 1008-1010 kg m<sup>-3</sup> at the surface to 1019 kg m<sup>-3</sup> at the bottom in 26m depth. Two days later the density is completely analog to the salinity again. The density also shows signs of mixing like the salinity, it increases with depths and has the same gradients like the salinity. In the surface layer the measured values are 1008-1010 kg m<sup>-3</sup> and at the bottom they are about

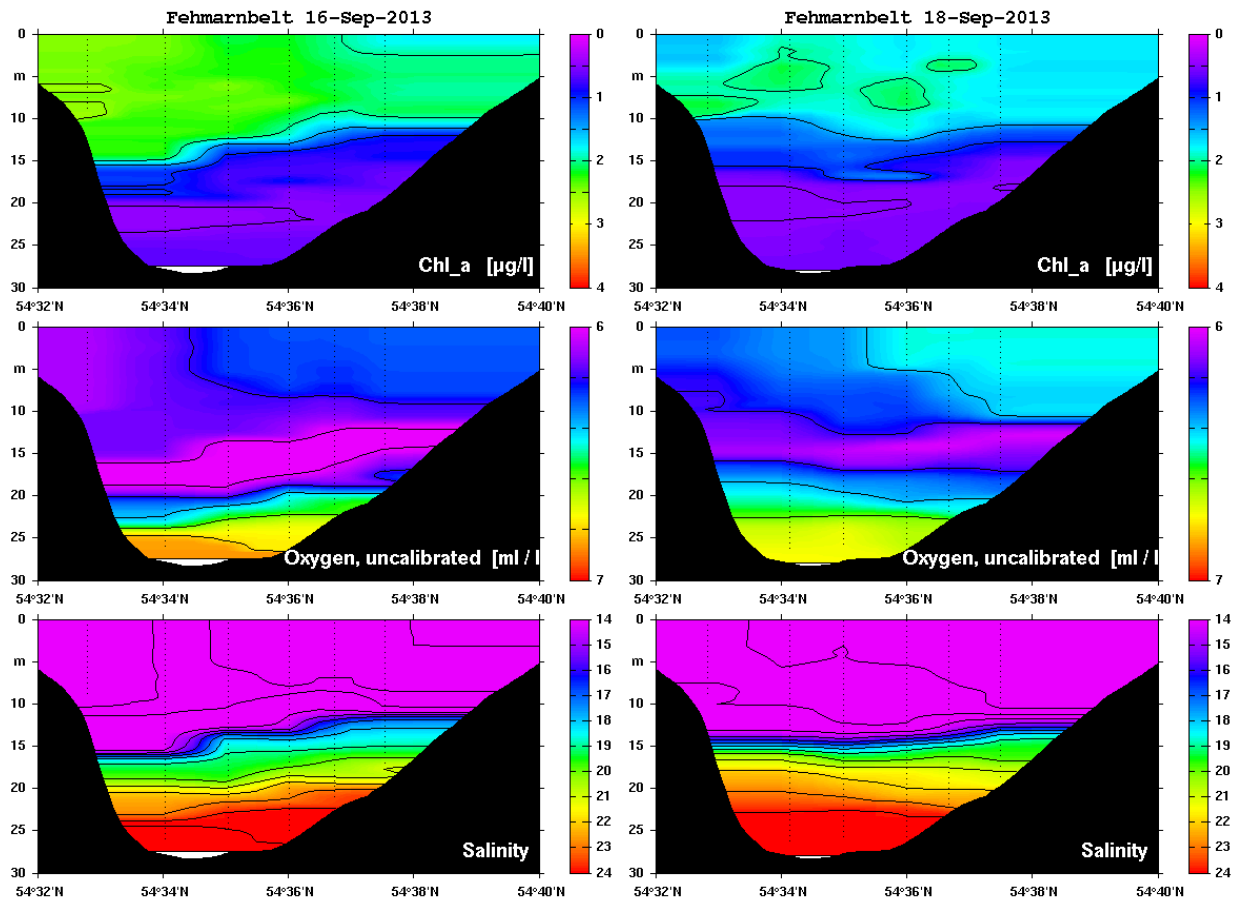


Figure 4.1: Chlorophyll, oxygen and salinity distribution along Fehmarn Belt. Left: 16. Sept. 2013, right: 18. Sept. 2013.

1019 kg m<sup>-3</sup> .

By looking at the oxygen distribution (Figure 3), it gets clear that the oxygen saturation is very small with only 6 to 6.2 mg/l in the first 20m below the surface. Just in 20-26m depth the saturation increases rapidly until it gets to 6.8 mg/l at the bottom. This also can be identified as a salty and oxygen-rich North Sea water inflow. In the figure two days later the oxygen distribution in the lower water columns from 12-26m stayed nearly the same like in the measurement two days before. In the surface layer an increase of oxygen can be found especially in the north. This section of the Baltic Sea seems to be strongly mixed. This could be a result of the interaction of ocean and atmosphere, e.g. by wind and the motion of waves. The fluorescence distribution shows similar gradients at certain depths like the salinity distribution with the difference that the fluorescence saturation decreases with depths. It starts with 2.5  $\mu l^{-1}$  in the surface layer and decreases with a strong gradient in 10-15m depth until it reaches only 0.5  $\mu l^{-1}$  at the bottom. Overall this can be attributed to the little solar irradiation in the depths. The fluorescence distribution two days later is also strongly mixed in the surface layer and significantly decreased to only 1.75  $\mu l^{-1}$  in average. Below 15m depth there are low measurement values and no significant change in the fluorescence distribution.

## Zonal section (L Section)

The zonal section (Fig. 4.2) shows the temperature, salinity, density, chlorophyll and oxygen distribution between Fehmarnbelt and Arkona Basin from September 23 to September 26 2012.

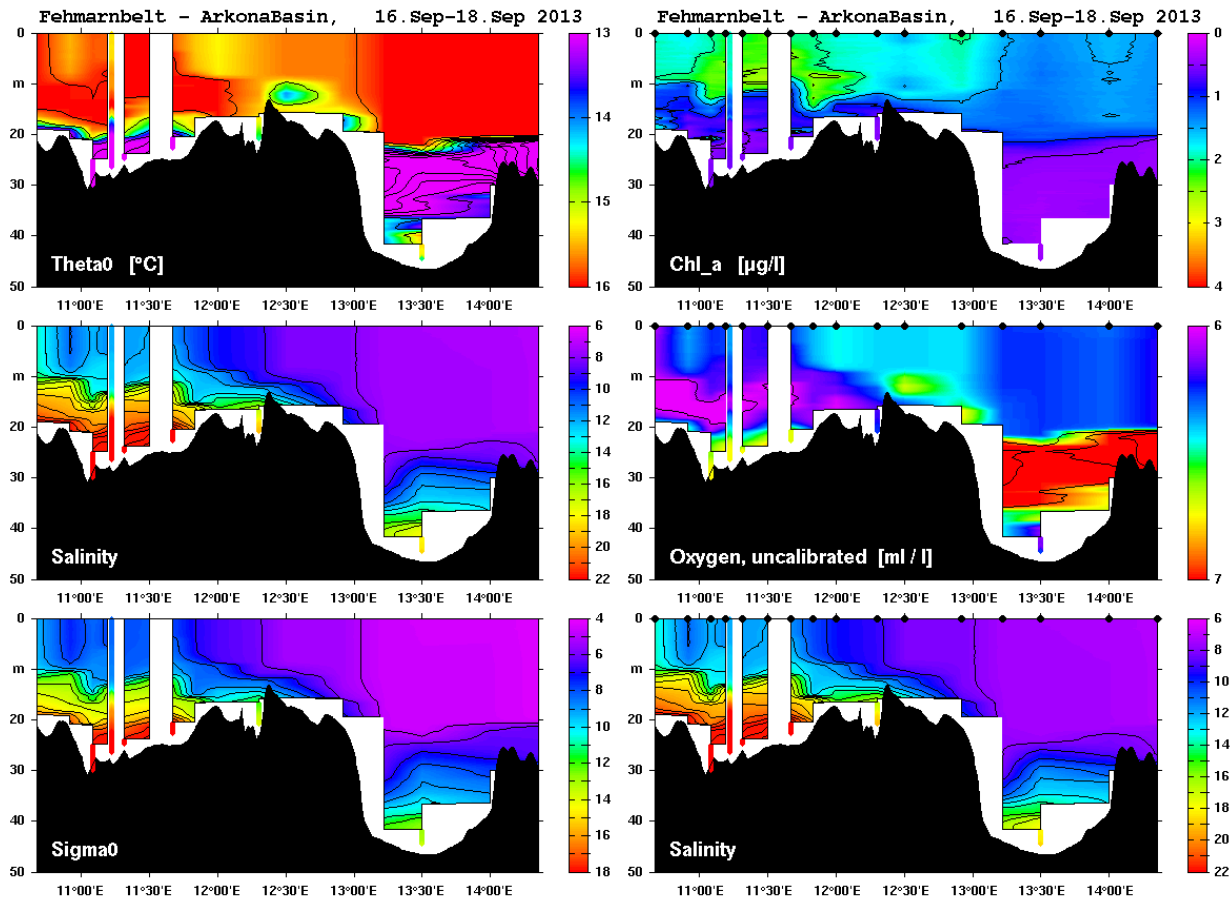


Figure 4.2: Potential temperature, salinity and potential density distribution along zonal section. 16. Sept. to 18. Sept. 2013.

In the zonal section from West to East the temperature distribution (Figure 4) within the upper 20m is nearly homogeneously 14 to 16°C. Just underneath 21m depth the water slowly cools down to 12°C in the west. In the east the water temperature quickly drops to 4-8°C with strong gradients in 21-23m depth. At a depth of 30m, the water is slowly getting warmer again until it gets to 14°C at the bottom in 40m depth. The salinity distribution differs even more from east to west. Westwards there is a nearly homogeneous surface layer with 11 to 14psu. At a depth of 10m the salinity slowly increases with weak gradients until it gets to 25 psu at the deepest part of the Fehmarnbelt. Eastwards the salinity is constantly at 8-10 psu in the first 30m and then slowly increases until it reaches 18psu at the deepest point in 42m depth. The salty North Sea water seems to stay at the deepest point in the Fehmarnbelt basin as shown in figure and reaches not further east in the Arkona Basin. The density distribution shows the same trend

as the salinity distribution with the same gradient in nearly the same depths. The water in the west with a maximum density of  $1019 \text{ kg m}^{-3}$  is significantly higher than in the east with a maximum density of only  $1013 \text{ kg m}^{-3}$ . In addition to this, the top layer in the west with an average density of  $1007 \text{ kg m}^{-3}$  is significantly higher than the average density of  $1005 \text{ kg m}^{-3}$  in the East. The oxygen distribution in the first 25 m, and therefore in the entire western part of the profile, is very little and homogeneous at 6 - 6.5 mg/l. Only in the Arkona Basin in the east, it increases underneath 20m depth with a strong gradient and has its maximum at 21 to 28m depth. There, the oxygen content is 9.5 mg/l throughout the east and 8 mg/l further west. From 30m depth, the oxygen content slowly drops again until only 6 - 6.5 mg/l at the bottom in 42m depth. The fluorescence is mostly present in the first 10m. In the West the fluorescence has a varying content of 2-2.5  $\mu\text{l}^{-1}$  and the East 1.5  $\mu\text{l}^{-1}$ . Underneath a depth of 10m, values are only sporadically higher than 1  $\mu\text{l}^{-1}$ .

## 4.2 Meteorological observations

To interpret the oceanographic data adequate, it is necessary to consult the meteorological weather conditions at the time of the oceanographic measurements. On the meteorological side we have recorded data from: DAVIS-Ship (true wind, velocity, dew point, water-temperature, global radiation, long-wave radiation), DWD-Data (absolute wind-velocity, absolute wind-direction, air pressure, air temperature, water-temperature) and the extracted data out of the psychrometer measurements (dew-point, air temperature, air humidity).

At the start of the cruise on 16th of September, the weather-map (fig.4.3) shows two low-pressure areas located in the northwest and southeast of the ship. In fig. 4.4 the true wind direction and speed can be seen. The Data, analyzed from DAVIS has a higher spread than the DWD data and shows higher wind speeds. The stable wind-direction with  $250^\circ$  for the first 24 hours that can be seen in the DWD-data lay perpendicular on the occlusion of the island-cyclone. The mild and relatively windy night from the 16th to the 17th of September might be a result of its influence. The Island-Low becomes weaker over the time of the cruise coupled with increasing pressure until the forenoon of the 17th September and distribute into different small low-pressure areas at Wednesday. In the second part of the cruise the influence of one of these little lows in the east of the ship increases leading to lower pressure and slow northerly winds. The route of the cruise is shown in fig. 3.1.

The second night had much lower temperatures and slower wind-velocities than the night before. The temperatures reach their deepest point at about  $10^\circ\text{C}$ . In general the water-temperatures are higher than the air-temperatures. They are discussed with the humidity in the following heat-flux section. In fig. 4.4 it can be seen, that the ideal time series of the short-wave radiation is disturbed by the cloudiness. On Monday two broken-cloud-effect peaks are conspicuous.

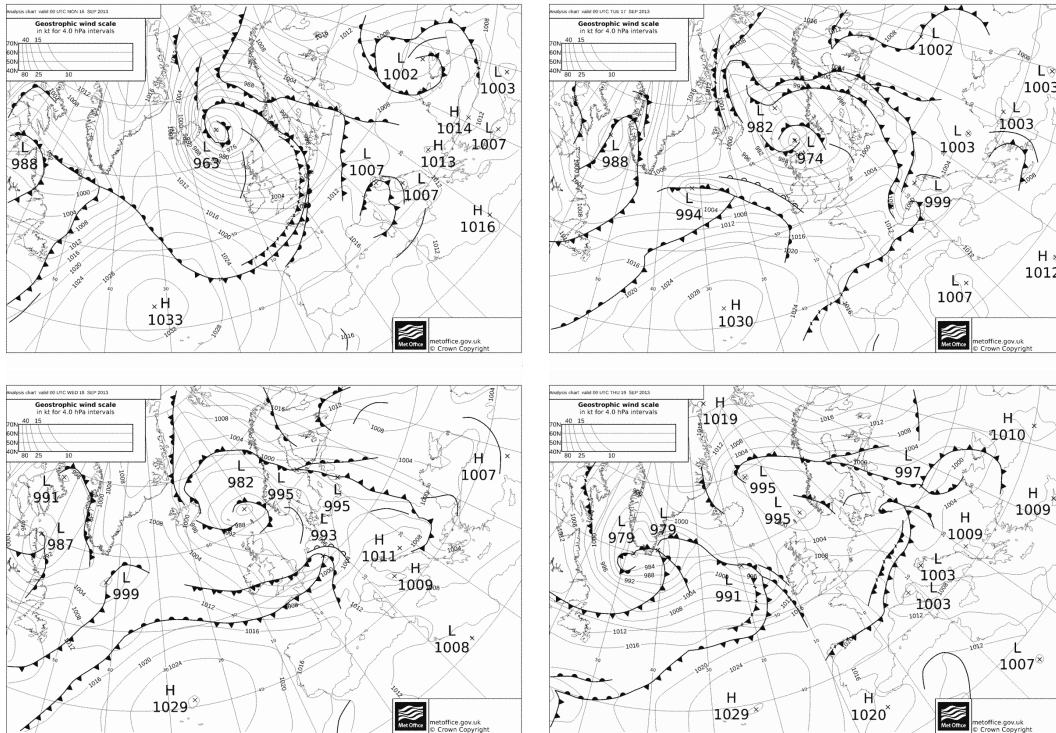


Figure 4.3: *Surface pressure analysis charts from MetOffice for the period September, 16 to September 19, 2013.*

## 4.2.1 Heat Fluxes

### Latent heat-flux:

The time series of the latent heat-flux is shown in fig.:4.5. Starting with a very high humidity and low wind velocities on Monday morning the latent heat-flux was very low. With increasing speed and decreasing humidity the atmosphere is able to absorb more water vapour and the latent heat-flux increases. Vice versa lower wind-speed and higher humidity reduces the latent heat-flux. The moisture and the velocity data are anti-correlated, so the latent heat-flux in general follows the shape of the wind-speed and the upside down moisture data. The latent heat-flux on Wednesday morning is much lower than on Tuesday, what may be lead back on to the decreasing strength of the Island-Low.

### Sensible heat-flux:

In fig.:4.5 the progress of the sensible heat-flux is shown. Influenced by the wind-speed, the sensible heat-flux is lower in the nights and shows the same difference between Wednesday and Tuesday morning, as the wind-velocity. Deviating from this is an abrupt decrease of the flux at Tuesday 13:00 attributed to a lower temperature gradient between water and atmosphere. The antecedent fifteen hours the ship was east of the Lolland-Rügen axis, related with warmer surface

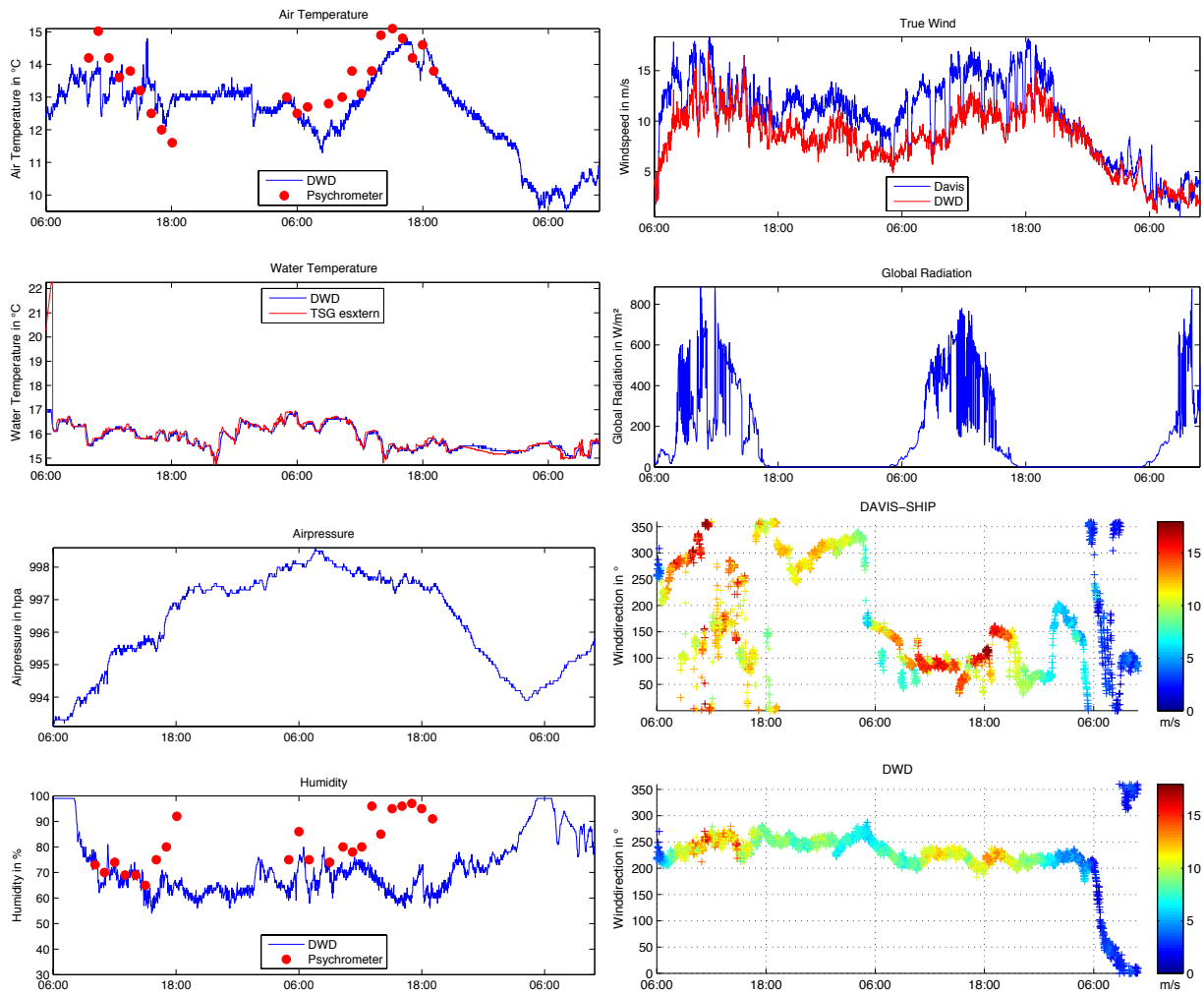


Figure 4.4: Air temp, true wind speed, water temperature, global radiation, air pressure, wind speed, humidity, true wind direction.

water. At Tuesday 13:00 the ship entered colder water at midday with higher air temperatures leading to a very low temperature difference. The sensible heat-flux is relatively high, because of the cold air over warm water in the beginning of autumn.

**Long-wave radiation:**

Lower sea-surface-temperatures (SST, for simplification the external TSG-sensor temperature was used, fig. 4.5) are related to lower long-wave radiation, whereas higher SSTs are coupled with higher radiation fluxes. At daytime the back-radiation is higher than at night. That is why the higher long-wave radiation related to higher SST during the day are reduced after the sun sets. The long-wave radiation is a flux that transports energy out of the water, forcing a negative sign.

**Net heat flux:**

The balance of all four fluxes (sensible and latent heat-flux, short- and long-wave radiation) is shown in fig.:4.5. During the day (about 8.00-16.00) net heat and radiation are transported into the water, whereas in the rest of the time heat and radiation are net transported into the atmosphere. The transport at daytime is about twice as high as the transport in the rest of the time. Here the differences between the single days are not very conspicuous. Only the transport into the atmosphere in the second night is a little bit higher. On Tuesday, where we have data for 24 hours, the net heat flux is  $-17.3Wm^{-2}$ , which means, that the ocean loses and the atmosphere gains heat during the cruise.

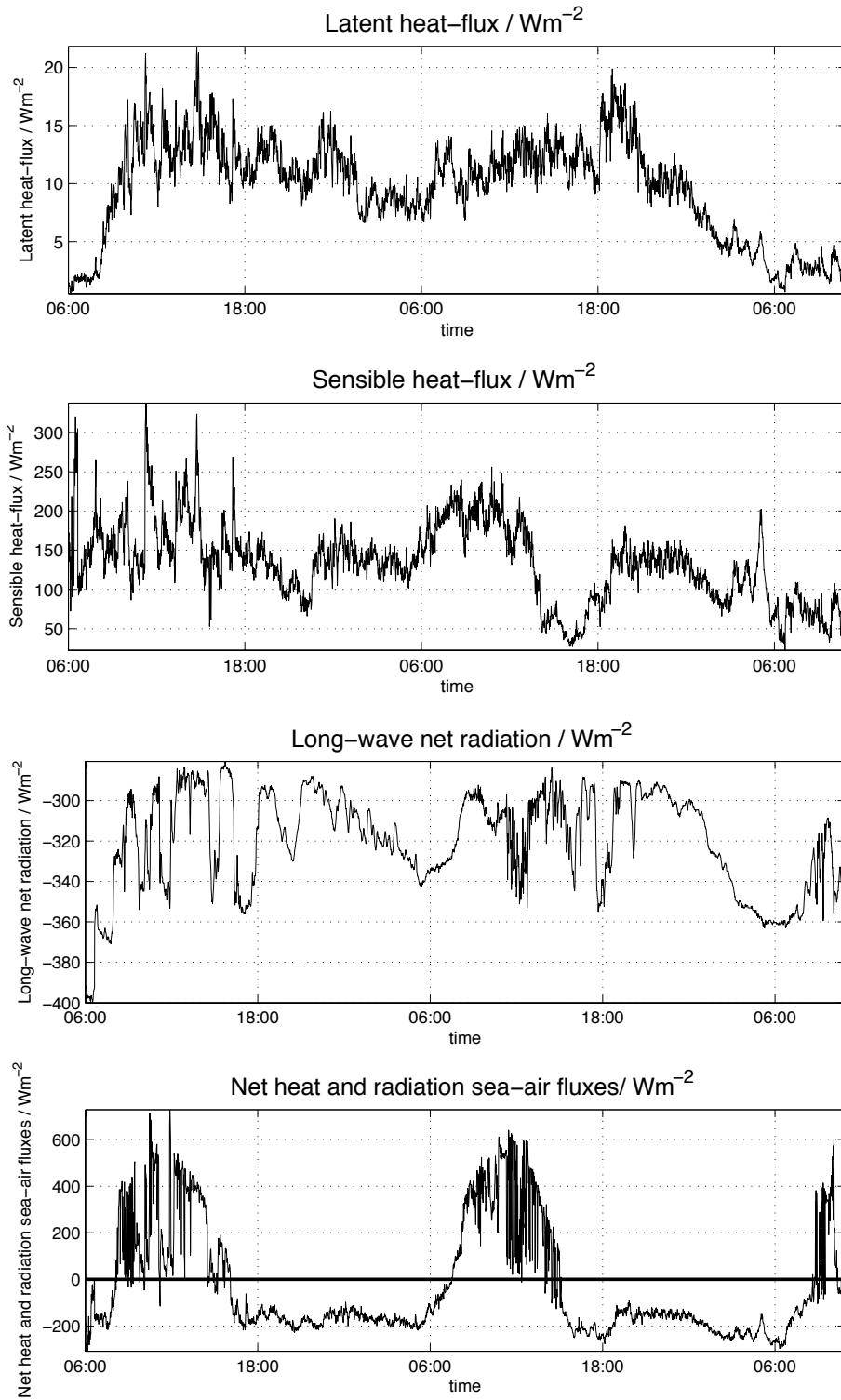


Figure 4.5: Various surface fluxes.

### 4.3 Mooring

The V431 is installed in the Speergebiet Marienleuchte since 2002. During A1423 the mooring was recovered on the 16. September 2014. Unfortunately the ground weight could not be recovered (the rope broke off, probably due to a problem with the steel thimble that was used. The RV Deneb (BSH) searched for the ground weight but could not detect it (11. Dec. 2013). A second attempt (11. February 2014) failed as well. It is very difficult to find the ground weight only.

Nevertheless, time series from the recoveries of the RCDP for the period 05. Dec. 2012 to 16. Sept. 2013 could be prepared. The time series of T/S/O<sub>2</sub> show a seasonal cycle. Interesting is that the oxygen content varies considerably between saturated in winter and nearly anoxic conditions by the end of the summer - also observed in the former deployment period. The currents show the expected flow structure of inflow at levels below about 18m and outflow above. Short term variability in the order of a couple of days regularly disturbs the flow field, caused by wind events.

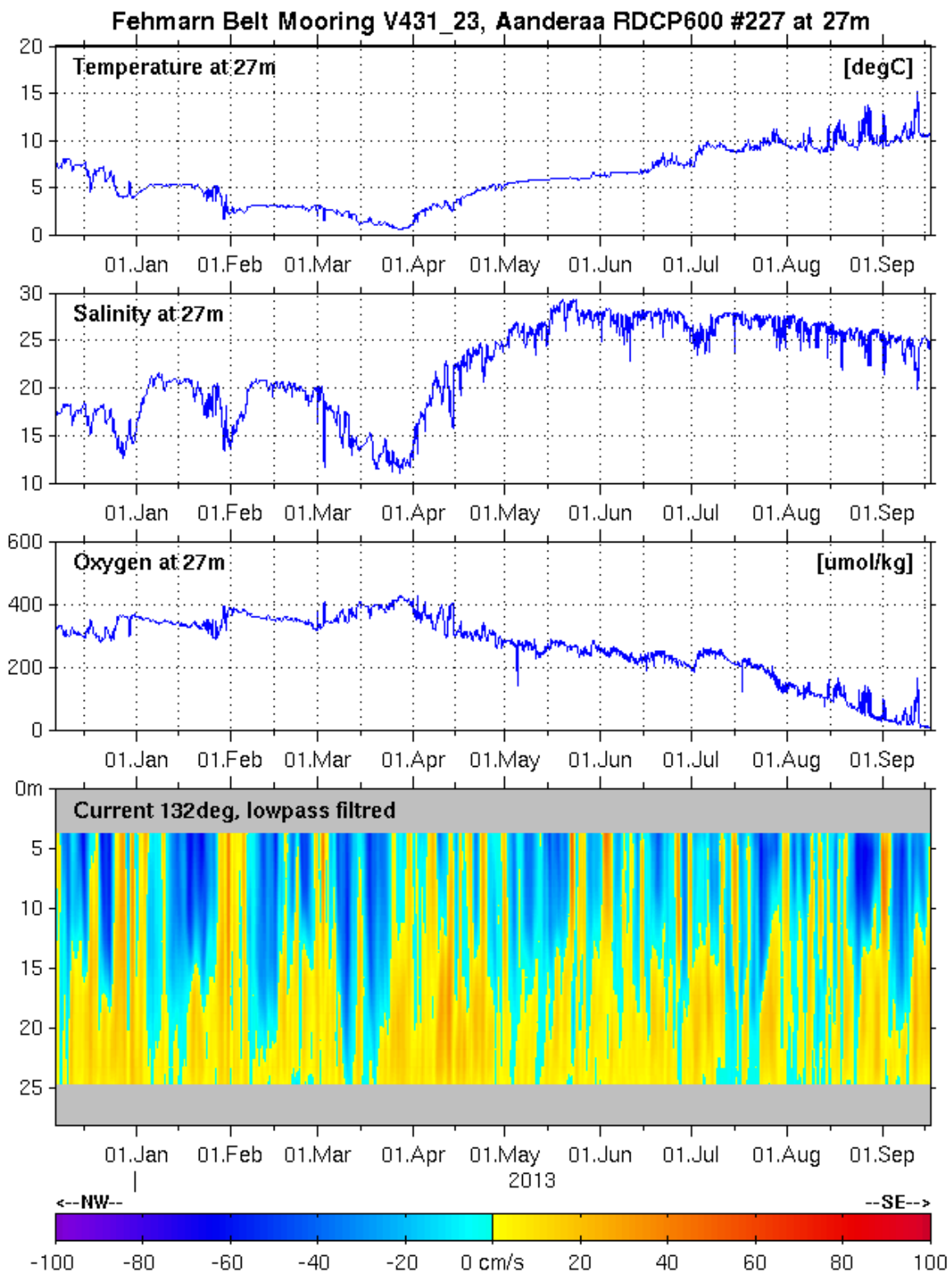


Figure 4.6: (from top to bottom) temperature, salinity, oxygen and current rotated in  $132^\circ$  from the RDCP 600 at V431 position at 28m water depth.

# Chapter 5

## Equipment/instruments

### 5.1 Technical: Mooring V431

Mooring deployment site V431 is located in the military zone of Marienleuchte at the southeastern opening of the Fehmarn Belt. Water depth is about 28m. V431 consists of a Aanderaa RDCP600, serial 227 with temperature (serial 2639, type:3621), conductivity (serial 85, type: 4019A), oxygen Optode (3830, serial 679) and a self containing T/S recorder of type SBE-MicroCat (serial number 2936). The ADCP and all other parameter logging was programmed for every hour, the MicroCat (not recovered yet) record every 15 minutes.

The Aanderaa RDCP600 is configured for current recordings in 1.5m depth cells covering the whole water column. So far no 100% successful deployment can be reported, and again we had a problem with the battery power during the deployment - as the battery seem to be not able to last long enough (1 year) although the battery calculator indicates. This could be due to the lower power availability of the lithium batteries in cold waters (nominal energy density is calculated against 20°C).

### 5.2 Salinometer Measurements

We used a Hydro-BIOS *CTD* probe to make our *CTD* measurements. It can be used online, sending acquired data to a deck command unit on board, connected to the probe under water via a single or multi-conductor cable, or offline, storing the data on an internal memory chip (16Mb). It records one data set per second (1Hz), which gives us a good resolution at a casting velocity of approximately  $0.1 \frac{m}{s}$ , which we mainly chose, because of rather shallow water depths in the Baltic Sea. The Hydro-BIOS probe can be used to a maximum depth of 3000m and measures temperatures between -2 to 32 °, with an accuracy of  $\pm 0.005^\circ$ , and conductivity between 0 and  $65 \frac{mS}{cm}$ , accuracy of  $\pm 0.001 \frac{mS}{cm}$ . We used three bottles with a capacity of 10 litres each attached to the rosette to take samples from various water depths to later compare and evaluate the measured salinities of our *CTD* casts with salinometer measurements. We used a Beckmann-salinometer with an accuracy of approximately  $\pm 0.002psu$  to determine the salinity of our *CTD* samples.

Due to the operation of salinity measurements with the *CTD* probe, which requires the use

of indirect parameters like temperature and conductivity to derive any given salt concentration, a constant calibration with a more precise instrument, the Beckmann-salinometer, under a much more controlled environment is needed.

In order to achieve this, water samples have been taken from various depths at every *CTD* station. One large (10 litres), clean sample taken at a greater depth at the beginning of the cruise served as a so-called *substandard* to prepare the apparatus and to identify a possible drift in the measurements over time.

The salinometer measurements started on day 2 of the cruise after a thorough introduction by chief scientist Dr. Johannes Karstensen and a calibration with *IAPSO standard sea water*. The correct handling of the salinometer depends on the avoidance of any foreign matter contaminating the bottles and its contents as well as on minimizing the amount of air bubbles sucked into the metering apparatus. Since the water is propelled around the system during measurements, intrusions like air bubbles would harm the ability to accurately set up the equipment or make it even impossible, due to a high oscillation of the reading. Another important factor influencing the accuracy and reproducibility of the measurements is temperature. To reach the best possible accuracy, sample temperatures must not vary by more than  $1K$ . To ensure this, samples had to sit inside the laboratory for at least a day so they all had the same temperature. Also, the salinometer itself had to be turned on at least an hour before the first measurement could be made. During our measurements, we realized that it was very hard to prevent bubbles from getting sucked into the apparatus. This became even harder when the vacuum pump stopped working properly, apparently a prominent issue with this particular device. It was fixed temporarily but quit again shortly after, preventing any more measurements and resulting in a rather slim collection of quality samples measured with the salinometer.

To further reduce errors, each sample was measured until at least two values differed by no more than  $0.01psu$ .

If we look at the difference between the *CTD* and salinometer measurements of salinity, we first have to evaluate a possible drift in the salinometer measurements (Fig. 5.1). For that we used the aforementioned substandard. By re-measuring this substandard after four different samples, assuming a constant salinity for this large sample and rejecting obviously wrong values (we found salinity values of over  $400psu$  in the provided datasets) we could detect a drift, produced by the salinometer itself. This drift could also be enhanced by fluctuating room temperatures in the laboratory. We determined the drift to be approx.  $-0.00614\frac{psu}{h}$  (assuming linearity) and a standard deviation of  $0.0351psu$  (though below std., we corrected the drift anyway).

We can then subtract this drift from all the salinometer measurements and therefor correct them (Fig. 5.2). We then use these corrected values to evaluate our *CTD* samples. We can safely assume the laboratory measurements to be the more accurate ones. This is because of the controlled environment the salinometer is in. With a rather constant room temperature and a drift detected and already subtracted, possible errors are small (Fig. 5.3) compared to those of *CTD* measurements. Also the fact that multiple measurements have been done on each sample further reduces differences.

<i>bottel No.</i>	86	88	628	157	207	154	1041	3	90	153	87	76	35
<i>station</i>	2	2	3	3	3	4	4	4	5	6	6	6	7
<i>sample</i>	4	5	1	2	3	1	2	3	2	1	2	3	1

<i>bottel No.</i>	174	170	33	173	172	3444	169	3443	27	43	82	92
<i>station</i>	7	7	8	8	8	9	9	9	10	10	11	11
<i>sample</i>	2	3	1	2	3	1	2	3	1	2	1	2

There are several reasons why the *CTD* probe is more prone to errors. For one, there's the time constant problem of the temperature sensor. The slow adaption ( $65ms$ ) of the sensor to changes in temperature can lead to salinity spikes in the *CTD* profile. Also, a pressure dependence of the sensors is possible, will be neglected in this evaluation though, due to rather shallow water depths in the Baltic Sea. Other factors such as the up and downward movement of the ship during sampling or turbulence around the rosette or the sensors could also affect the *CTD* measurements. The *CTD* measurements provide vertical profiles of salinity and temperature and with the values collected with the salinometer we can evaluate the quality of the *CTD* measurements and possibly detect a systematic deviation from the true values.

Given the fact that by numerous measurements, discarding flawed data and the general higher precision of a Beckmann-salinograph compared to on-board equipment of a *CTD*, one can safely assume that the achieved values (Fig. 5.2) are trustworthy and critically better.

Observing Fig. 5.5 it's obvious that there is a trend for the *CTD*-probe to deliver values that are too high. Although the average offset is at  $0.77psu$  still considerable lower than one standard deviation ( $1.16psu$ ), 10 data points still exceed it (by up to  $2.59psu$ ). Furthermore the aforementioned trend is by no means consistent and isolated glitches below real salinity may occur as well.

Apart from that an average deviation of  $0.77psu$  to what we have to assume to be the actual salinity is too inexact regardless. *CTD*-salinity-data may serve as a good guideline but must not be taken at face-value uncondinonally.

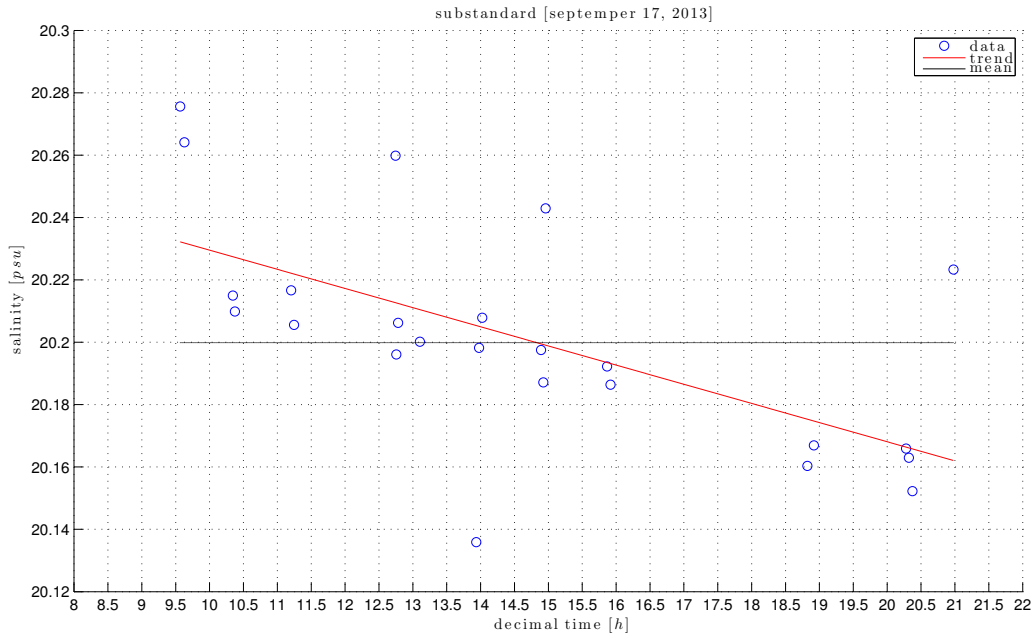


Figure 5.1: Measurements of substandard-samples as a function of time, (blue: linear fit; red: mean value; black:substandard)

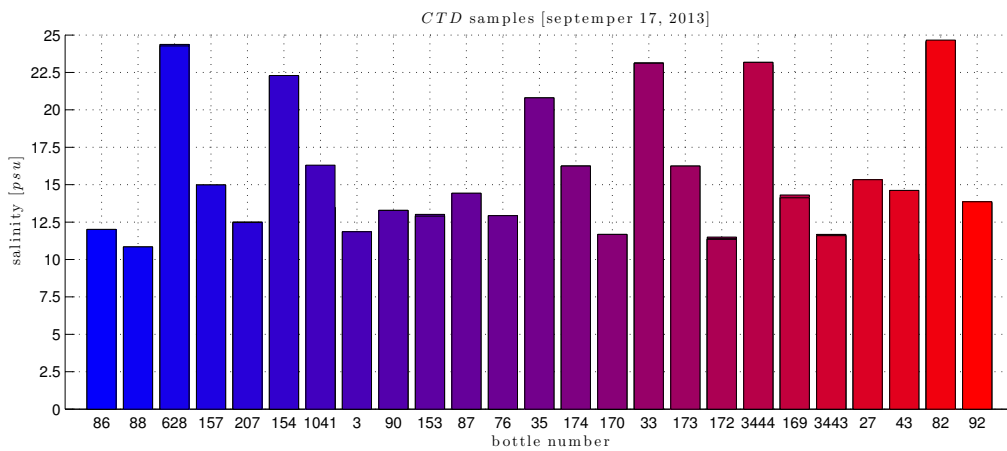


Figure 5.2: drift-corrected CTD-samples measured with salinograph [Bottle numbers are sorted by time they were taken. They cover the samples taken between stations 2 and 11. Later stations couldn't be checked due to the salinograph breaking down.]

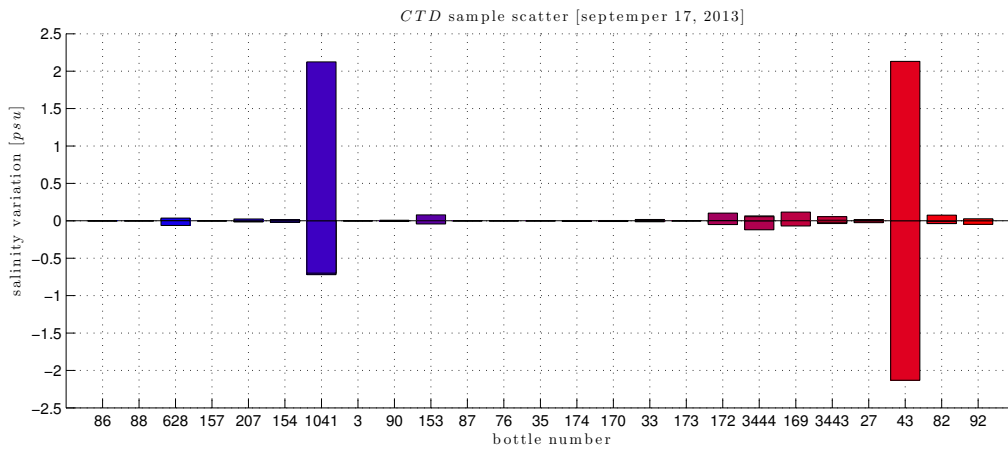


Figure 5.3: Scatter of *CTD*-sample measurements in relation to their respective means. For most samples the differences between multiple readings seems reasonable good. Large deviations as for instance at  $N_o$ . 1041 and 43 are possibly caused by single measurements being compromised by handling errors (i. e. air bubbles). Those values are going to be neglected and will not be used for comparison to *CTD*-data and only those values differing by less than  $0.01psu$  for each respective bottle will be selected for further use.

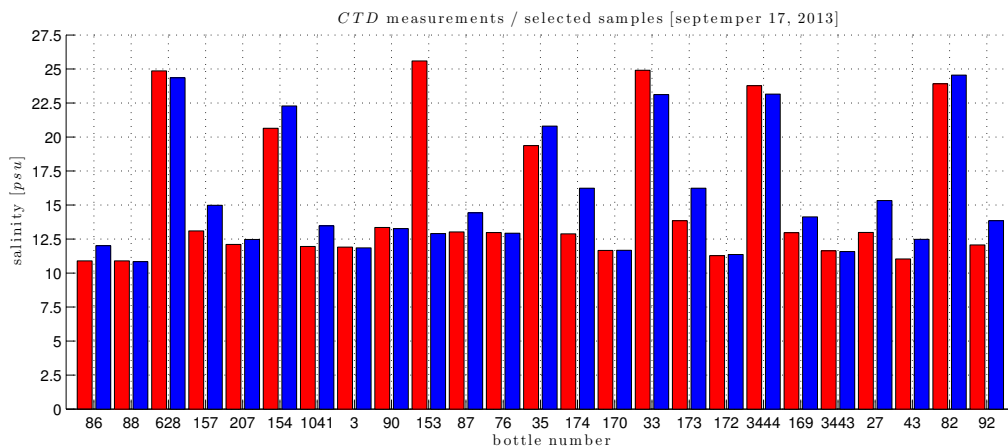


Figure 5.4: Sample values  $S_{Sal}$ . by salinograph (blue) and in-situ measurements  $S_{CTD}$  by *CTD*-probe at the position each sample was taken (red)

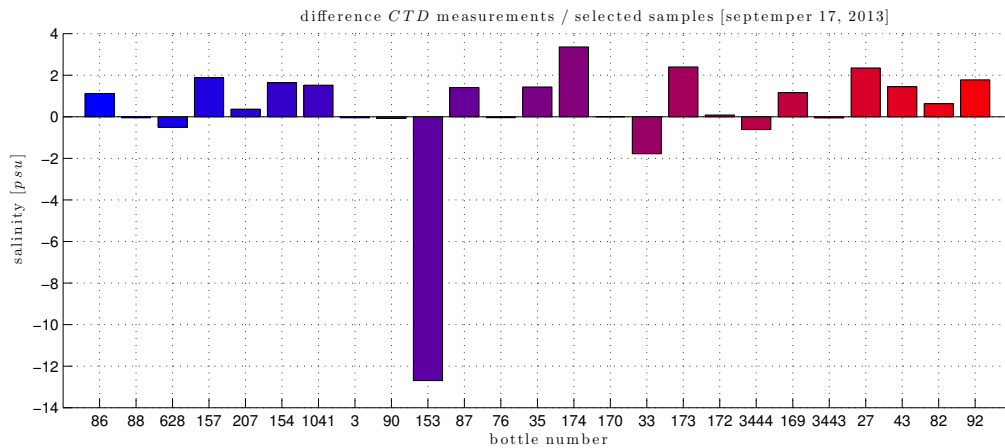


Figure 5.5: *difference  $S_{CTD} - S_{Sal}$  of the values shown in Fig. 5.4* [So on average the *CTD*-probe provides salinities that are  $0.27psu$  too high according to this data. If we neglect sample *No.* 153, which obviously suffered from a major error from the *CTD*s sensor as the salinograph results appear valid, the average offset of the *CTD* rises to  $0.77psu$ . The standard deviation is  $2.93psu$  (with #153), respectively  $1.16psu$  (without #153).]

## **5.3 Underway Measurements**

### **5.3.1 WERUM**

FS ALKOR has a new central data collection system from WERUM. The system worked perfect during the cruise and facilitated our work in providing on-line cruise map, a downloadable station book as well as export of relevant data. The WERUM is a substitute for the former 'DATADIS' system that caused a lot of trouble during the last years and we are very happy that this new WERUM system was installed on FS ALKOR.

### **5.3.2 Navigation**

FS ALKOR has a GPS navigational system as well as a gyro compass available and distributed via WERUM. The WERUM map viewer allowed following the cruise track online.

### **5.3.3 Meteorological Data**

Since March 2006 FS ALKOR is equipped with a so-called automatic weather station which should acquires the basic meteorological parameters (air temperature, wind speed and direction, wet-temperature, humidity, air-pressure). Shortwave radiation is also measured. Long wave radiation is recorded with an EPLAB (Eppley Laboratory, Inc.) Precision Infra-red Radiometer (Model PIR).

### **5.3.4 Echo sounder**

The ER 60 SIMRAD echo sounder was activated during the cruise.

### **5.3.5 Thermosalinograph**

The SBE37 Thermosalinograph on FS ALKOR is installed in the boats hull and is constantly measuring temperature and electric conductivity. To provide the on-board computer with the right temperature-data there is an additional temperature sensor at the inlet at about 3m depths on the ships bow. This is necessary because the water temperature rises while it's flowing through the boats hull.

The salinity, calculated by the TSG through conductivity of the seawater, is compared to the CTD measurements in equal depths (Fig. 5.6). The mean difference between these two shows a few mistakes with no general offset which could be caused by a small time difference between the measurements or the spatial disparity.

For the temperature comparison between TSG data and CTD data an offset is much smaller (Fig. 5.6) and mostly positive. Reasons could be a small general difference in depth during the measurements or warmer water from the upper layer flowing down the boats hull into the inlet causing the temperature there to rise. But the difference is very small so we assumed temperature measurements as correct.

Another method we applied to get results as accurate as possible was to take TSG-samples and measure their salinity with the salinometer. The probes corresponded with the measured TSG data (Fig. 5.7). Unfortunately the salinometer did not work anymore after the second day and until then mostly CTD probes were measured and we could only compare a few TSG probes with the salinometer.

Completing the calibration we compared the TSG salinity data with the SVT data (Fig. 5.7). The SVT uses the salinity to calculate sound velocity. The two graphics match but the SVT salinity is usually higher by 4 to 6 salinity units. Because the TSG data does not show this offset compared to CTD and salinometer data, we have to assume that the mistake is in the SVT measurements.

From earlier cruises on FS ALKOR we expected a small positive offset in the salinity measurements, but it is not possible to generalize the differences to be always positive or negative direction. Because of that no correction has been applied to the data.

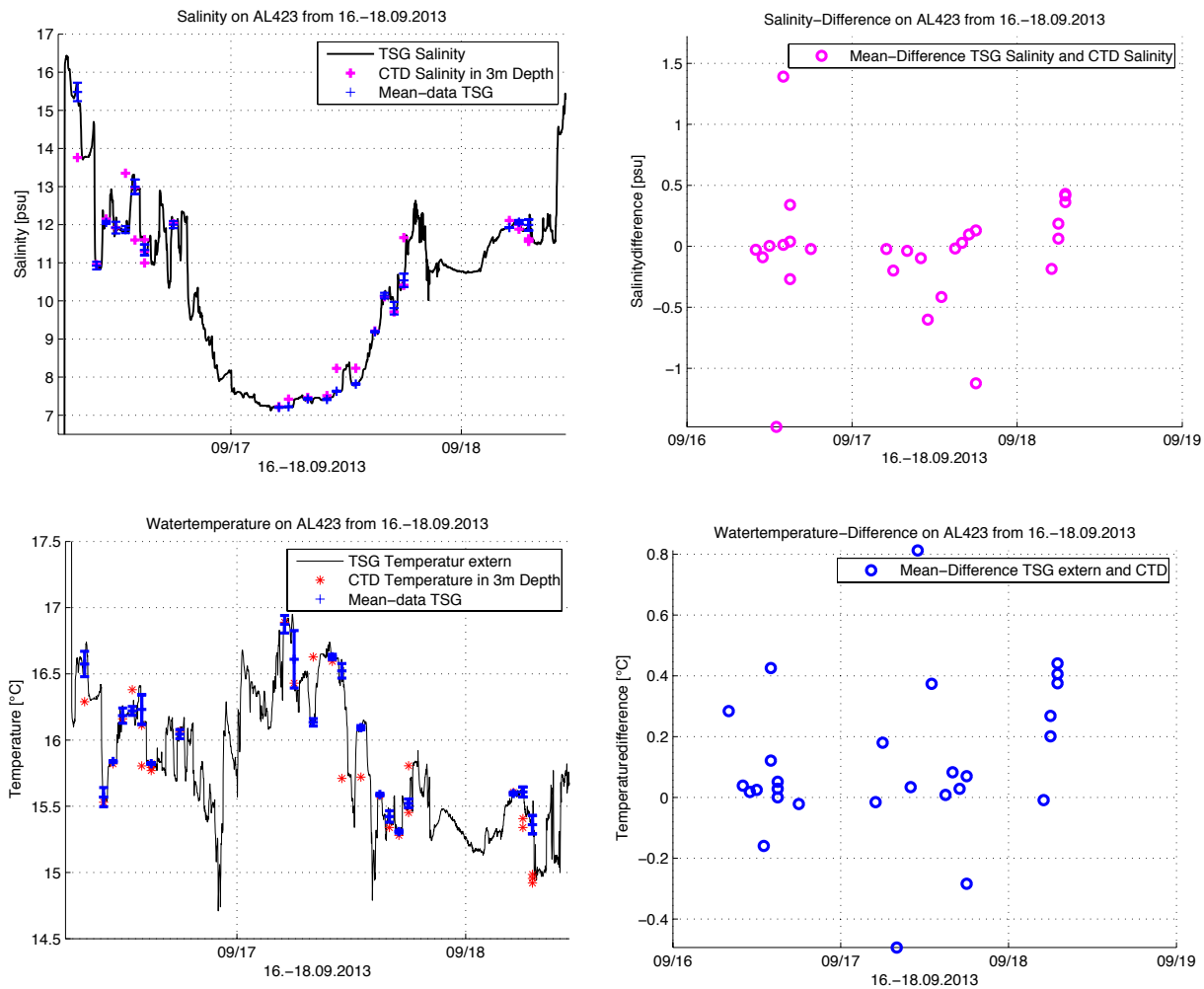


Figure 5.6: TSG and CTD data comparison.

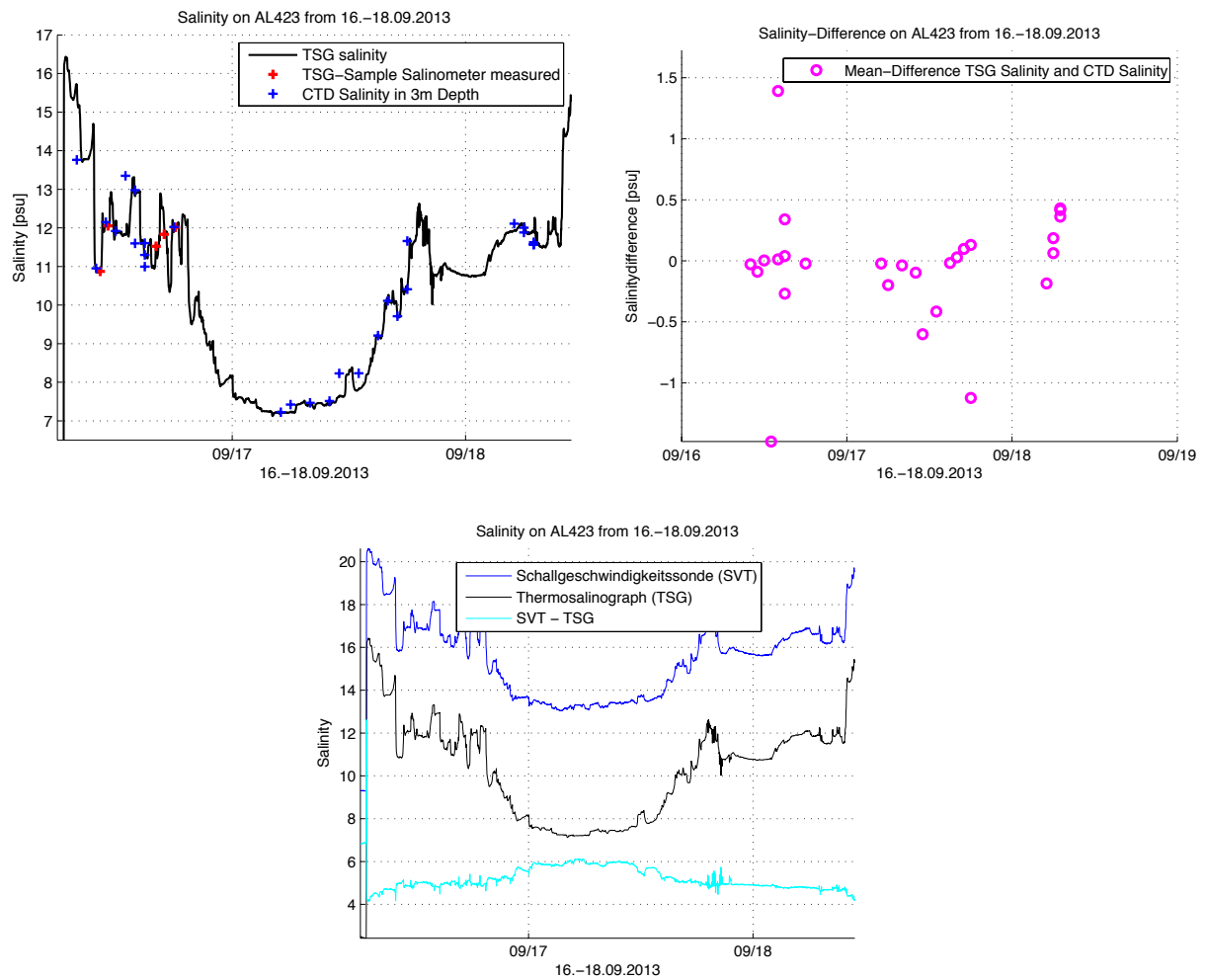


Figure 5.7: TSG data and salinometer as well as sound velocity derived salinity.

### **5.3.6 Vessel mounted ADCP**

A 600kHz workhorse ADCP from RD Instruments was mounted in the ships hull. The vmADCP is used with bottom tracking mode. Navigational data (including ships heading) is available via a THALES 3011 dGPS system.

# Chapter 6

## Acknowledgement



A big thank to N. Hechler (master), J. Mairon (chief engineer), C. Gräber (1st off.) and all crew members of FS ALKOR for a successful and comfortable cruise.

# Chapter 7

## Appendix

### Station table

St. Latitude Longitude waterdepth year month day time

1	54.5642	10.6711	20	2013	9	16	8.92
2	54.6078	10.9177	20	2013	9	16	10.17
3	54.5915	11.0838	31	2013	9	16	11.02
4	54.5082	11.3116	26	2013	9	16	12.18
5	54.5467	11.1641	10	2013	9	16	13.73
6	54.5672	11.1852	28	2013	9	16	14.20
7	54.5840	11.2088	27	2013	9	16	14.60
8	54.6002	11.2244	26	2013	9	16	15.02
9	54.6123	11.2417	23	2013	9	16	15.38
10	54.6257	11.2577	20	2013	9	16	15.75
11	54.4498	11.5013	25	2013	9	16	18.12
12	54.6339	14.3485	31	2013	9	17	5.00
13	54.7818	14.0000	38	2013	9	17	6.68
14	54.9156	13.5000	46	2013	9	17	8.83
15	54.8619	13.2189	43	2013	9	17	10.33
16	54.8088	12.9174	22	2013	9	17	11.78
17	54.6344	12.5014	18	2013	9	17	13.83
18	54.5337	12.3019	22	2013	9	17	15.00
19	54.3893	12.1831	20	2013	9	17	16.20
20	54.3584	12.0023	18	2013	9	17	17.05
21	54.3504	11.8339	22	2013	9	17	18.80
22	54.3505	11.6673	25	2013	9	17	18.60
23	54.5471	11.1626	11	2013	9	18	5.92
24	54.5690	11.1876	28	2013	9	18	6.43
25	54.5833	11.2076	27	2013	9	18	6.85
26	54.6000	11.2265	27	2013	9	18	7.28
27	54.6113	11.2417	24	2013	9	18	7.65
28	54.6249	11.2579	20	2013	9	18	7.97